Intra-abdominal desmoplastic small round cell tumors: CT and FDG-PET/CT findings with histopathological association

JINGJING CHEN[1], ZENGJIE WU[2], BINBIN SUN[3], DACHENG LI[4], ZHENGUANG WANG[4], FANGJUN LIU[5] and HUI HUA[6]

[1]Department of Radiology, The Affiliated Hospital of Qingdao University, Shandong 266003; [2]Department of Positron Emission Tomography/Computed Tomography, Qingdao Center Medical Group, Shandong 266042; [3]Department of Diagnostic Ultrasound, Affiliated Zhucheng People's Hospital, Weifang Medical University, Shandong 262200; [4]Department of Positron Emission Tomography/Computed Tomography, The Affiliated Hospital of Qingdao University, Shandong 266003; [5]Institute of Plastic Surgery, Weifang Medical University, Shandong 261042; [6]Department of Otorhinolaryngology - Head and Neck Surgery, The Affiliated Hospital of Qingdao University, Shandong 266003, P.R. China

Received December 21, 2014; Accepted January 8, 2016

DOI: 10.3892/ol.2016.4421

Abstract. Desmoplastic small round cell tumors (DSRCTs) are rare and aggressive malignant tumors. The aim of the present study was to analyze computed tomography (CT) and fluorodeoxyglucose positron emission tomography (FDG-PET)/CT imaging features of intra-abdominal desmoplastic DSRCT, and investigate the association of these features with histopathological results. The present study was a retrospective investigation of 4 patients with DSRCT. All patients underwent CT and dynamic CT, and 1 additionally underwent FDG-PET/CT scanning. Following a tumor resection, routine hematoxylin and eosin staining, and immunostaining, were performed and evaluated. Multiple large abdominopelvic masses were identified in all 4 patients; however, no indications of their site of origin were demonstrated. CT revealed soft-tissue masses with patchy foci of hypodense lesions. Contrast-enhanced CT revealed slightly or moderately heterogeneous enhancement of the lesions. Other observations from these patients included calcification (n=2), peritoneal seeding (n=3), hepatic metastasis (n=3), retroperitoneal lymphadenopathy (n=3) and ascites (n=2). FDG-PET/CT revealed multiple nodular increased FDG uptake in the abdominopelvic masses, and in the liver and peritoneum in 1 case. Intra-abdominal DSRCT demonstrated significant diagnostic characteristics on plain and contrast-enhanced CT. Multiple, bulky soft-tissue masses inside the peritoneal cavity, particularly in male adolescents and young adults, should be considered as potential cases of DSRCT. FDG-PET/CT techniques may be utilized to aid the staging of tumors.

Correspondence to: Dr Hui Hua, Department of Otorhinolaryngology - Head and Neck Surgery, The Affiliated Hospital of Qingdao University, 16 Jiangsu Road, Qingdao, Shandong 266003, P.R. China
E-mail: huahuisky@163.com

Professor Jingjing Chen, Department of Radiology, The Affiliated Hospital of Qingdao University, 16 Jiangsu Road, Qingdao, Shandong 266003, P.R. China
E-mail: chenjingjingsky@126.com

Key words: abdomen, desmoplastic small round cell tumor, computed tomography, positron emission tomography

Introduction

Desmoplastic small round cell tumors (DSRCTs) are rare and aggressive malignant tumors with a poor prognosis, which were initially described by Gerald and Rosai in 1989 (1). Currently, ~200 cases have been reported in the literature (2). DSRCT primarily affects young males between the ages of 15-25 years (3,4). The most commonly affected region is the pelvis, with other sites including the omentum, the retroperitoneal space and the mesentery (3-6).The manifestations of DSRCT are non-specific, and patients typically present with vague abdominal or pelvic discomfort, including abdominal pain and/or distension, ascites, constipation and urinary disorders (2,6,7). Histologically, DSRCT is characterized by well-defined nests or clusters of small, round tumor cells embedded in an abundant, desmoplastic stroma (8,9). DSRCT is associated with the reciprocal chromosomal translocation t(11:22)(p13;q12), which involves the EWSR1 and WT1 genes (9). The prognosis of patients with DSRCT is poor, with a mean survival time of <30 months (10). Postoperative radiotherapy and chemotherapy are reported to have no survival advantage, and successful surgical excisions are extremely rare (10,11). Previous studies of DSRCT have focused on its pathological features (1,8,9), however, few studies have assessed the computed tomography (CT) and fluorodeoxyglucose positron emission tomography (FDG-PET)/CT results of this disease (3,4,6,10-14). The present study aimed to characterize the CT and FDG-PET/CT imaging results of 4 DSRCT patients, and to associate these observations with the pathological findings.

Materials and methods

Patients. The present study retrospectively reviewed 4 patients with DSRCT, clinically diagnosed by histopathology, who were treated at the Affiliated Hospital of Qingdao University Medical School (Shandong, China) between January 1, 2009, and March 31, 2011. All patients were male, with a mean age of 22.25 years (range, 14-31 years). Clinical manifestations included an abdominal mass (n=2), abdominal pain and distension (n=1), and jaundice (n=1).

CT scanning and image analysis. Plain and triple-phase dynamic CT scans were performed using a 64-slice CT scanner (SOMATOM Sensation Cardiac 64; Siemens, Munich Germany) in 3 patients or using a 16-slice CT scanner (Brightspeed; GE Healthcare Bio-Sciences, Pittsburgh, PA, USA) in 1 patient. The CT scan included a section thickness of 5 mm, a pitch of 1.375:1 and a field of view of 248x330 mm. Patients were administered 1L of 3% meglumine diatrizoate (Shanghai Xudong Haipu Pharmaceutical Co. Ltd., Shanghai, China), an oral contrast agent, a total of 30 min prior to examination. Patients were additionally administered 100 ml iopromide (Ultravist 300; Bayer HealthCare Pharmaceuticals, Berlin, Germany), a non-ionic iodinated contrast material. All patients initially underwent plain CT scanning, followed by triple-phase CT examination that included arterial, portal and delayed phases. Contrast material was administered at a rate of 3.0 ml/sec with an automatic power Ultravist® 300 injector (Bayer AG, Berlin, Germany). Enhanced CT was performed in the arterial, portal and delayed phases, with a delay time of 25, 60 and 120 sec, respectively, following initiation of injection of the contrast materials. All CT images were reviewed retrospectively by 2 professional radiologists each with >20 years experience in abdominal CT studies. The imaging results were evaluated for tumor location, shape, size, number, margin, density and intensity of contrast enhancement. When compared with adjacent tissue, the tumor density on plain CT was defined as low density, isodensity or high density. The intensity of enhancement, when performing contrast-enhanced CT, was classed as no, mild, moderate or distinct enhancement.

FDG-PET/CT scanning and image analysis. FDG-PET/CT was performed in 1 patient using a dedicated PET/CT system (Discovery ST 16; GE Healthcare Bio-Sciences). The patient was instructed to fast for at least 6 h prior to injection of ^{18}F-FDG. The patient's blood glucose level was <11.1 mmol/l (normal range, 4.2-6.9 nmol/l). Following intravenous injection of ^{18}F-FDG (0.14 mCi/kg), the patient lay comfortably in a quiet and dark room for 1 h. PET, CT and fused PET/CT images of the whole body were reviewed by 2 nuclear medicine physicians. The imaging results were evaluated for tumor location, shape, size, number, margin, density and maximum standard uptake value (SUVmax) of all lesions.

Histopathology. The tumors in 3 patients were resected totally (2 cases) or partially (1 case), and CT-guided needle biopsy of the tumor was performed in the fourth patient. All cases demonstrated no complications following tumor resection. Gross examination, including analysis of tumor shape, size, number, margin and capsule wall, was conducted in all specimens prior to routine histological evaluation. The samples were fixed in formalin (Liaocheng Jianhua Chemical Products Co., Ltd., Shandong, China), embedded in paraffin (Taicang City Haotian Technology Co., Ltd., Jiangsu, China), and stained with hematoxylin and eosin (Labest Biotechnology Co., Ltd, Beijing, China). A BX43 microscope (Olympus Corporation, Tokyo, Japan) was used to observe specimens. Immuno-histopathological examinations were additionally performed, which included assays for mouse anti-human anti-cluster of differentiation (CD)99 monoclonal antibody (catalog no., ZM-0296), mouse anti-human anti-neuron specific encolase (NSE) monoclonal antibody (catalog no., ZM-0203), mouse anti-cytokeratin monoclonal antibody (catalog no., ZM-0069), mouse anti-epithelial membrane antigen (EMA) monoclonal antibody (catalog no., ZM-0095), mouse anti-desmin monoclonal antibody (catalog no., ZM-0091) and mouse anti-vimentin monoclonal antibody (catalog no., ZM-0260) (dilution, 1:200; Beijing Zhongshan Golden Bridge Biotechnology Co., Ltd., Beijing, China).

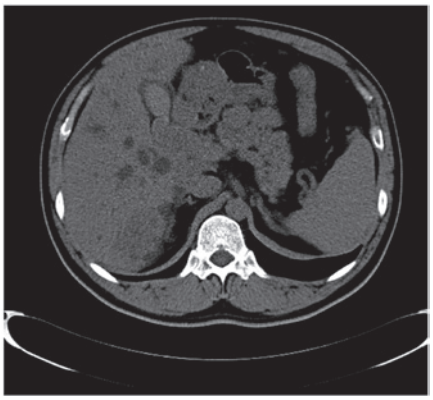

Figure 1. Plain computed tomography image at the axial plane showing multiple intra-abdominal nodules and masses with soft tissue density and well-defined margins, and dilation of the intrahepatic bile due to a hepatic hilar mass.

Results

CT imaging findings. CT images revealed multiple intra-abdominal nodules and/or masses with soft tissue density in all patients, and these masses exhibited vague margins with adjoining organs. The tumor size was variable, with a maximum size of 170x170 mm (Fig. 1). Multi-node and patchy calcifications were observed inside the foci in 2 cases (Fig. 2). Nodular thickening of the peritoneum in 3 patients was noted as mild or moderate enhancement in the contrast-enhanced CT. Multiple concurrent masses in the liver were identified in 3 patients, with a maximum tumor size of 117x118 mm. Although the majority of these masses were located close to the superficial layer of the liver, 1 patient presented with a mass occupying the hepatic hilum, which caused dilation of the intrahepatic bile duct (Fig. 1). A total of 3 patients exhibited multiple nodules with soft tissue density surrounding the retroperitoneal abdominal aorta. Contrast-enhanced CT of the tumor masses and nodules appeared as mild to moderate edge enhancement of the lesion, however, a lower density and no appearance of enhancement was observed within the centre of the larger lesions (Figs. 2 and 3). Furthermore, 1 patient

with a large tumor in the pelvic cavity demonstrated dilation of the proximal ureters, renal pelvicalyses and hydronephrosis due to pressure on the bilateral ureters (Fig. 2). Furthermore, 2 patients exhibited a low level of abdominal ascites.

FDG-PET/CT imaging findings. PET/CT imaging revealed multiple nodular foci of FDG uptake in the abdominopelvic cavity, liver and peritoneum (Fig. 4). The SUVmax of all masses ranged between 4.0 and 12.9.

Intraoperative results. Large intra-abdominal masses were observed in all 3 patients who underwent tumor resection, and these masses adhered to the omentum and adjacent organs. Numerous firm nodules of variable size were distributed on the surface of the abdominal viscera and omentum. In addition, multiple firm masses were identified inside the liver in 2 patients, 1 of whom was treated with a complete resection of the intrahepatic tumor.

Histological results and immunohistochemistry findings. In terms of gross appearance, the surgically removed tumor masses from 3 patients were poorly circumscribed, grey-white in color and had a crisp texture. The majority of tumor masses exhibited areas of tissue necrosis in the centre of the lesion, and a number of tumor nodules had a greyish-yellow appearance, similar to rotting flesh.

Microscopically, the DSRCT cells varied in size and spherical or ovoid in appearance; however, there were additionally a small number of spindle-shaped cells. The tumor cells had reduced cytoplasm, and acidophilic and hyperchromatic nuclei. Clusters of these undifferentiated tumor cells infiltrated the surrounding dense connective tissue, and appeared as solid nests that were well-defined and had differing shapes and sizes (Fig. 5).

Immunohistochemistry revealed positive results for NSE, CK, and EMA expression in the DSRCT cells from all 4 patients, whereas only 2 cases demonstrated positive staining for either CD99 or desmin. In addition, vimentin was strongly expressed in only 1 patient.

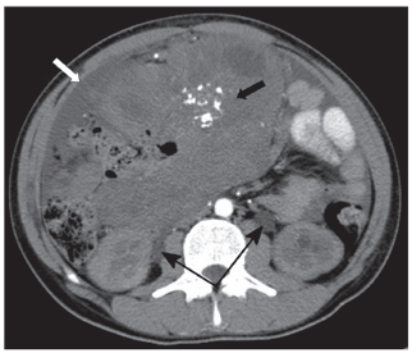

Figure 2. Contrast-enhanced computed tomography image demonstrating multiple nodules and masses with mild to moderate enhancement, multinodal and patchy calcification inside the foci (thick black arrow), dilation of the proximal ureters, renal pelvis and calyces (thin black arrows), and ascites (white arrow).

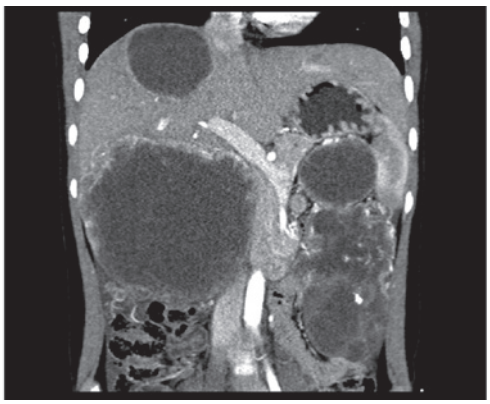

Figure 3. Coronal plain computed tomography image showing multiple large tumor masses with edge enhancement inside the abdominal cavity and liver.

Discussion

DSRCT is a rare and highly malignant neoplasm, which commonly arises in the peritoneal cavity and has a poor prognosis. It is now widely recognised to be a member of the family of small round blue cell tumors (12).

Previous studies have indicated that DSRCT primarily occurs in male adolescents and young adults (male:female, 4-5:1) (12,15,16), however, a case has been reported in a 65-year-old woman (17). The clinical findings are non-specific, and the disease most commonly presents as abdominal pain and distension, ascites and hydronephrosis (3-15). In the present study, the patients (male adolescents and young adults with an age range of 14-31 years) complained of abdominal pain and distension, and the presence of an abdominal mass, with the exception of 1 patient, who presented with jaundice due to oppression of the hepatic bile duct by tumor masses.

DSRCT shows a higher rate of occurrence on serosal surfaces, where it appears as single or multiple nodular masses on the surface of intra-abdominal organs (12). The tumor may additionally occur in the omentum, with involvement of the surrounding viscera. Other common areas of involvement are the scrotum, lungs, chest wall, skull, pleura, mediastinum, thighs, soft tissues, bones, sinonasal regions, ovaries, kidneys and parotid glands, as well as the retroperitoneal space (12).

DSRCT frequently disseminates along the peritoneum or invades neighbouring organs inside the peritoneal cavity. Local metastasis of the tumor most commonly occurs in the liver, but may be observed in abdominal and pelvic lymph nodes, with varying degrees of ascites (5,12). Although the hematogenous metastasis of tumor cells is rare, there have been numerous reports of metastasis to remote organs, including the lungs, pleura, ilium and scrotum (9,12,14).

In the present study, multiple intra-abdominal nodules and masses were noted by the appearance of soft tissue density on CT scanning and variable tumor sizes in all 4 patients, and 3 cases showed involvement of the pelvic cavity. These 3 patients had exhibited nodular thickening of the peritoneum and adhesion between the tumor and omentum when the tumor occurred in the peritoneal cavity. Disseminated tumor masses on the visceral surfaces were frequently multifocal and of varying sizes. Multiple concurrent masses in the liver were observed in 3 patients, featuring a maximum tumor size of 117x118 mm. Although the majority of masses were located close to the superficial layer of the liver, 1 patient presented with a mass that occupied the hepatic hilum, which caused

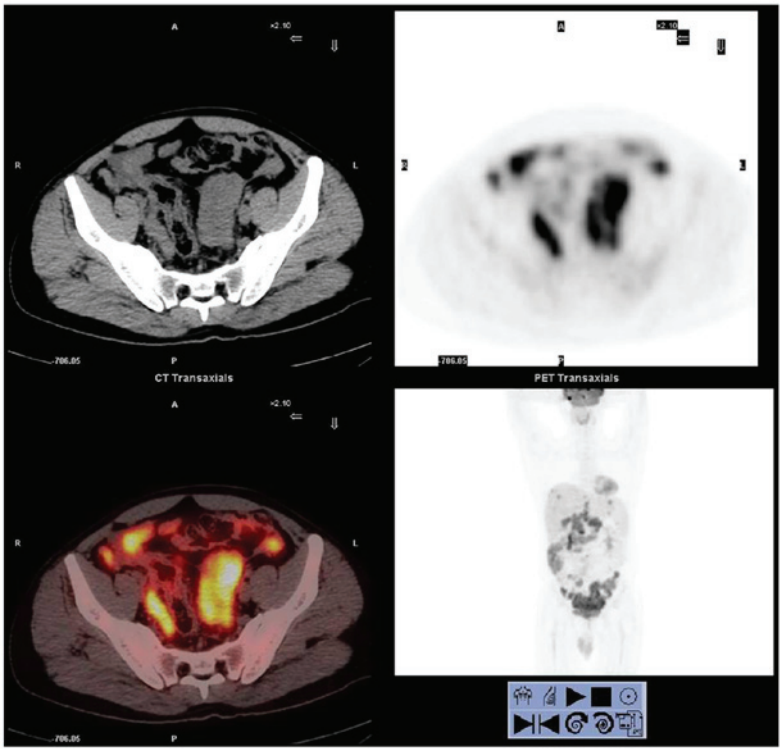

Figure 4. Fluorodeoxyglucose positron emission tomography/computed tomography image showing hypermetabolic abdominopelvic masses, liver metastases and peritoneal disease (maximum standard uptake value, 12.9).

dilation of the intrahepatic bile duct. The remaining 3 patients presented with slightly enlarged retroperitoneal lymph nodes. The patient with a large mass in the pelvic cavity showed dilation of the proximal ureters, renal pelvicalyses and hydronephrosis due to pressure on the bilateral ureters. In addition, 2 patients exhibited low levels of abdominal ascites.

CT scanning is the most frequently used method for the diagnosis of abdominal DSRCT (7). In plain CT, DSRCT appears as multiple and lobulated soft tissue masses in the abdomen, pelvic cavity or retroperitoneal space, with no clear site of origin (4). The tumors are of varying sizes (up to 40 cm in diameter) and appear with non-homogeneous density on CT images. The central areas of the foci result in a diverse range of low-density images, which correspond to hemorrhagic necrosis in gross specimens (14). Under contrast-enhanced CT, DSRCT appears with mild-to-moderate or heterogeneous image enhancement, although larger nodules or masses show only edge enhancement (6,7,14). Pickhardt *et al* (6) reported that 7/9 patients showed a lower density change in the centre of the tumor. The results of the present study are consistent with this previous study. Contrast-enhanced CT scanning of tumor masses and nodules revealed mild or moderate edge enhancement of the lesion, and lower density or no appearance of enhancement within the central area of larger lesions in the abdominal cavity and liver, which represented the area of necrosis in the gross specimens. Multinodal and patchy calcifications were observed inside the foci in 2 cases, as reported previously (3,9).

Numerous CT findings of diagnostic importance exist for DSRCT, including an adolescent age of onset, calcification of the tumor tissue, extensive involvement of the peritoneum and the absence of a clear site of origin. Zhang *et al* (3) and Bellah *et al* (12) suggested that the involvement of the retrovesical region may be valuable for the diagnosis of DSRCT. In the present study, 3 patients were diagnosed with DSRCT with involvement of the peritoneal and retrovesical regions.

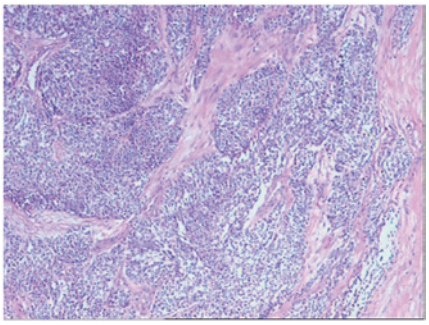

Figure 5. Histological appearance of the tumor mass showing small undifferentiated round cells surrounded by dense desmoplastic stroma, and formation of tumor cell nests that are well defined and of varying sizes (hematoxylin and eosin staining; magnification, x100).

FDG-PET/CT has a significant role in tumor staging and the identification of occult lesions that cannot be detected by CT or magnetic resonance imaging (MRI) (3,18). In the present study, masses with high FDG uptake and an SUVmax of 4.0-12.9 were indicative of malignancy. Compared with CT, FDG-PET/CT is able to reveal smaller metastases and can distinguish tumors from fibroses by whole-body metabolic imaging (3). PET/CT may be used for staging of DSRCT, and is an improved tool compared with CT or MRI (3,10). Additional studies utilizing FDG-PET/CT imaging are required.

Previous studies utilizing CT and FDG-PET/CT imaging in abdominal DSRCT are rare, therefore, little diagnostic

experience is available for clinicians (10,12). The radiological differential diagnosis for DSRCT is complicated by other abdominal and retroperitoneal tumors, including rhabdomyosarcoma, peritoneal leiomyosarcoma, mesothelioma, intra-abdominal desmoid tumor, primitive neuroectodermal tumors (PNETs), lymphoma and neuroblastoma (6,7,12). Rhabdomyosarcoma is primarily observed in infants (70% of cases occur in children aged <10 years) (19). Although these tumors may involve the peritoneum (~10%), typical nodules and masses are generally smaller compared with DSRCT, and calcification of tumor tissue is rarely observed (7,12). Peritoneal leiomyosarcoma typically affects women aged >24 years, however, DSRCT tends to occur in male adolescents (12). Leiomyosarcoma frequently appears as multiple well-defined nodules or lumps inside the peritoneal cavity or along the mesenterium (12). These tumors are prone to metastasis, primarily by hematogenous or lymphatic routes, although it is difficult to observe implantation metastases in the abdominal wall. Malignant mesothelioma rarely occurs in patients aged <20 years (20). This tumor accounts for ~15% of tumors involving the peritoneum, and is typically complicated by high levels of ascites. An intra-abdominal desmoid tumor is a rare, benign proliferation of fibrous tissue, which is typically solitary or associated with Gardner's syndrome (12). Intra-abdominal desmoid tumors that occur inside the pelvic cavity, retroperitoneal space or on the abdominal wall frequently manifest as single or multiple masses, with identical or reduced density compared with normal muscle tissue. These masses rarely show necrotic or cystic alterations, even inside large tumor masses (12). Furthermore, the absence of metastases is of differential diagnostic value in DSRCT patients. PNETs primarily affects adolescents and young adults, and is a highly aggressive tumor (12). Although the CT characteristics of PNETs are similar to those of DSRCT, the occurrence of tumor calcification is rare in PNETs (12). Lymphoma, unlike DSRCT, frequently occurs in middle-aged men, and manifests as enlarged lymph nodes in the abdominal cavity and retroperitoneal space during the early stages of the disease (12,21). By contrast, in its early stages, DSRCT frequently appears as a solid mass with no sign of lymph node enlargement (7,12). In addition, a distinguishing feature of lymphoma is the occurrence of spleen enlargement prior to tumor infiltration. Tumor calcification is also rarely observed in lymphoma. Neuroblastoma commonly affects infants, with 79% of patients aged <4 years (average age, 22 months), and typically appears as a single, paravertebral mass (12).

In conclusion, DSRCT is a rare and highly malignant neoplasm, which typically affects male adolescents and young adults. CT results of abdominal DSRCT are relatively characteristic and may assist with diagnosis. The CT imaging characteristics include, but are not limited to, multiple soft-tissue masses in the abdominal or pelvic cavity or retroperitoneal space, no clear site of origin, mild or moderate edge enhancement under contrast-enhanced CT, multinodal and patchy calcification of the tumor, adjoining organ involvement, and implantation metastases of the abdominal wall and/or hepatic metastasis. When a tumor with these characteristics is identified, particularly in adolescents and young adults, a diagnosis of DSRCT should be suspected. FDG-PET/CT may have a significant role in tumor staging.

References

1. Gerald WL and Rosai J: Case 2. Desmoplastic small cell tumor with divergent differentiation. Pediatr Pathol 9: 177-183, 1989.
2. Briseño-Hernández AA, Quezada-López DR, Corona-Cobián LE, Castañeda-Chávez A, Duarte-Ojeda AT and Macías-Amezcua MD: Intra-abdominal desmoplastic small round cell tumour. Cir Cir 83: 243-248, 2015 (In Spanish).
3. Zhang WD, Li CX, Liu QY, Hu YY, Cao Y and Huang JH: CT, MRI, and FDG-PET/CT imaging findings of abdominopelvic desmoplastic small round cell tumors: Correlation with histopathologic findings. Eur J Radiol 80: 269-273, 2011.
4. Kis B, O'Regan KN, Agoston A, Javery O, Jagannathan J and Ramaiya NH: Imaging of desmoplastic small round cell tumor in adults. Br J Radiol 85: 187-192, 2012.
5. Mainenti PP, Romano L, Contegiacomo A, Romano M, Casella V, Cuccuru A, Insabato L and Salvatore M: Rare diffuse peritoneal malignant neoplasms: CT findings in two cases. Abdom Imaging 28: 827-830, 2003.
6. Pickhardt PJ, Fisher AJ, Balfe DM, Dehner LP and Huettner PC: Desmoplastic small round cell tumor of the abdomen: Radiologic-histopathologic correlation. Radiology 210: 633-638, 1999.
7. Chouli M, Viala J, Dromain C, Fizazi K, Duvillard P and Vanel D: Intra-abdominal desmoplastic small round cell tumors: CT findings and clinicopathological correlations in 13 cases. Eur J Radiol 54: 438-442, 2005.
8. Kim HJ, Sohn BS, Kwon JE, Kim JY and Park K: ThinPrep cytological findings of desmoplastic small round cell tumor with extensive glandular differentiation: A case study. Korean J Pathol 47: 182-187, 2013.
9. Dufresne A, Cassier P, Couraud L, Marec-Bérard P, Meeus P, Alberti L and Blay JY: Desmoplastic small round cell tumor: Current management and recent findings. Sarcoma 2012: 714986, 2012.
10. Ben-Sellem D, Liu KL, Cimarelli S, Constantinesco A and Imperiale A: Desmoplastic small round cell tumor: Impact of F-FDG PET induced treatment strategy in a patient with long-term outcome. Rare Tumors 1: e19, 2009.
11. Nathan JD, Gingalewski C and Salem RR: Intra-abdominal desmoplastic small round cell tumor. Yale J Biol Med 74: 287-293, 1999.
12. Bellah R, Suzuki-Bordalo L, Brecher E, Ginsberg JP, Maris J and Pawel BR: Desmoplastic small round cell tumor in the abdomen and pelvis: Report of CT findings in 11 affected children and young adults. AJR Am J Roentgenol 184: 1910-1914, 2005.
13. Kim JH, Goo HW and Yoon CH: Intra-abdominal desmoplastic small round-cell tumor: Multiphase CT findings in two children. Pediatr Radiol 33: 418-421, 2003.
14. Tateishi U, Hasegawa T, Kusumoto M, Oyama T, Ishikawa H and Moriyama N: Desmoplastic small round cell tumor: Imaging findings associated with clinicopathologic features. J Comput Assist Tomogr 26: 579-583, 2002.
15. Gerald WL, Miller HK, Battifora H, Miettinen M, Silva EG and Rosai J: Intra-abdominal desmoplastic small round-cell tumor. Report of 19 cases of a distinctive type of high-grade polyphenotypic malignancy affecting young individuals. Am J Surg Pathol 15: 499-513, 1991.
16. Roberts P, Burchill SA, Beddow RA, Wheeldon J, Cullinane C and Lewis IJ: A combined cytogenetic and molecular approach to diagnosis in a case of desmoplastic small round cell tumor with a complex translocation (11;22;21). Cancer Genet Cytogenet 108: 19-25, 1999.
17. Gao DX, Liao SL, Shi XJ and Hui ZY: Desmoplastic small round cell tumor: A report of 5 cases. Clin Exp Pathol 16: 353-356, 2000.
18. Magnan H, Abramson SJ, Price AP, Grewal RK, Merchant MS, LaQuaglia MP and Meyers PA: Positron emission tomography for response assessment in desmoplastic small round cell tumor. J Pediatr Hematol Oncol 35: e190-e193, 2013.
19. Chung CJ, Bui V, Fordham LA, Hill J and Bulas D: Malignant intraperitoneal neoplasms of childhood. Pediatr Radiol 28: 317-321, 1998.
20. Haliloglu M, Hoffer FA and Fletcher BD: Malignant peritoneal mesothelioma in two pediatric patients: MR imaging findings. Pediatr Radiol 30: 251-255, 2000.
21. Johnson KA, Tung K, Mead G and Sweetenham J: The imaging of Burkitt's and Burkitt-like lymphoma. Clin Radiol 53: 835-841, 1998.